Intelligent Weld Manufacturing: Role of Integrated Computational Welding Engineering

S. A. David, Jian Chen, Brian T. Gibson and Zhili Feng

Abstract A master welder uses his sensory perceptions to evaluate the process and connect them with his/her knowledge base to take the necessary corrective measures with his/her acquired skills to make a good weld. All these actions must take place in real time. Success depends on intuition and skills, and the procedure is labor-intensive and frequently unreliable. The solution is intelligent weld manufacturing. The ultimate goal of intelligent weld manufacturing would involve sensing and control of heat source position, weld temperature, weld penetration, defect formation and ultimately control of microstructure and properties. This involves a solution to a problem (welding) with many highly coupled and nonlinear variables. The trend is to use an emerging tool known as intelligent control. This approach enables the user to choose a desirable end factor such as properties, defect control, or productivity to derive the selection of process parameters such as current, voltage, or speed to provide for appropriate control of the process. Important elements of intelligent manufacturing are sensing and control theory and design, process modeling, and artificial intelligence. Significant progress has been made in all these areas. Integrated computational welding engineering (ICWE) is an emerging field that will aid in the realization of intelligent weld manufacturing. The paper will discuss the progress in process modeling, microstructure, properties, and process control and automation and the importance of ICWE. Also, control and automation strategies for friction stir welding will be discussed.

Keywords Intelligent · Weld manufacturing · Sensing · Control
Automation · Weld pool · Geometry · Convection · Solidification
Integration · Modeling · Friction stir welding

S. A. David (✉) · J. Chen (✉) · B. T. Gibson · Z. Feng (✉)
Oak Ridge National Laboratory, Oak Ridge, TN, USA
e-mail: standavid@charter.net

J. Chen
e-mail: chenj2@ornl.gov

Z. Feng
e-mail: fengz@ornl.gov

S. Chen et al. (eds.), *Transactions on Intelligent Welding Manufacturing*,
Transactions on Intelligent Welding Manufacturing,
https://doi.org/10.1007/978-981-10-7043-3_1

1 Introduction

Welding is a multibillion dollar industry used extensively in the construction of buildings, bridges, aircraft, ships, automobiles, and electronics. In recent years welding has emerged as a multidisciplinary activity that involves a large number of variables and that requires knowledge of basic science and engineering. In the last four decades, significant advances have been made in taking welding from a job shop technology to a highly automated, computer-oriented technology [1–7]. To meet the demands of quality and productivity is a continuing challenge. This is where intelligent weld manufacturing comes into play. Worldwide significant amount of work is being done in intelligent weld manufacturing [8].

"Intelligent manufacturing is real-time-based optimization through the entire value chain." Welding is ideally suited for intelligent manufacturing. It involves sensing and control of the heat source, position, weld defect formation, and ultimately microstructure and properties. This involves solution to a problem with many highly coupled and nonlinear variables in welding. The trend is to use intelligent control. This enables the user to choose a desired end factor such as penetration and productivity to drive the selection of process parameters such as current, voltage, and speed to provide for appropriate control of the process. In other words, intelligent welding aims at controlling for microstructure properties and performance of the welded parts. Chen has discussed the frame work for the science and technology for intelligent weld manufacturing [9]. Important elements of intelligent weld manufacturing are sensing and control design, process modeling, and artificial intelligence. The ultimate goal of intelligent weld manufacturing is to produce high-quality welds with increased productivity. To achieve this, it is necessary to have a thorough knowledge and understanding of four key elements: (1) process and process modeling, (2) microstructure, (3) properties, and (4) process control and automation. Mathematical modeling and simulation are integral parts of these elements. Details about the four elements are found in the published literature [10, 11]. Figure 1 shows the importance and integration of these elements. A wealth of information is available about these four elements in the Proceedings of a series of two International Conferences, namely, Trends in Welding Research and Mathematical Modeling of Weldability, held in recent years [10, 11]. The proceedings of these conferences contain a wealth of knowledge and information on intelligent control and automation. Although significant advances are being made in all these four areas, to integrate them successfully for a process that is highly coupled with a large number of variables is a major challenge. An approach to solving this problem is integrated computational welding engineering (ICWE). ICWE is an approach to design and produce welds in materials and by methods linking process models. ICWE is a major part of intelligent weld manufacturing. Another emerging field is integrated computational materials engineering (ICME). Both ICWE and ICME are engineering disciplines that speed up process development by integrating materials design, fabrication, and performance using computational process.

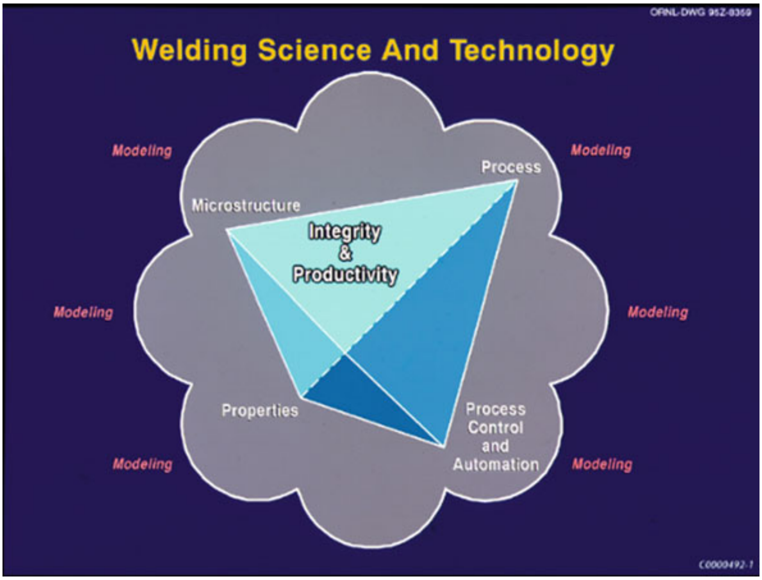

Fig. 1 Integration of process, microstructure, properties and process control and automation [10]

The paper will address the role of ICWE and ICME models in advanced intelligent weld manufacturing. It will address the progress made in various aspects of ICWE and ICME, most importantly in welding processes, microstructure and properties, and process control and automation. Current state-of-the-art of process modeling, microstructure and properties modeling, integration of various models, and sensing and control will be discussed. The paper will also address control and automation strategies for friction stir welding.

2 Process Modeling

In this section, recent advances in processes and process modeling will be described.

2.1 Weld Pool Dynamics and Geometry

Two of the most important parameters to control in automation are penetration and weld geometry. During welding, as the heat source interacts with the metal, several physical processes occur (e.g., melting, evaporation of elements, solution of gases, solidification, phase transformation residual stresses). It is important to understand the physical processes and their interactions to develop ICWE and intelligent weld manufacturing. Direct observation of the process is difficult, time consuming, and expensive because of the complexities, the large number of variables, and the presence of plasma. A solution is to model and simulate the process using equations of conservation of mass, momentum, and energy with appropriate boundary conditions.

Significant advances have been made in calculating the weld pool geometry [12–27] since the earlier Rosenthal analysis of heat flow in welds [28, 29], which was an analytical and a conduction model. Weld pool heat flow and fluid flow are recognized to be critical in the development of the shape and size of the weld pool and the macrostructure and microstructure of the weld. Current models address coupled conduction and convection problems to predict weld pool geometry. Of the various heat transfer models, the ones with convection play a major role in determining weld pool geometry and penetration. Convection in the weld pool is driven by surface tension, buoyancy, and electromagnetic forces [15, 17, 18, 30–36]. In addition, aerodynamic drag force due to plasma stream is also thought to be a factor [36]. Various forces are shown schematically in Fig. 2 [36]; convection due to surface tension is the dominant force contributing to fluid flow in the weld pool. The presence of a significant temperature gradient on the weld pool surface leads to spatial gradient of surface tension, also known as Marangoni stress, which contributes to convection in the weld pool. Buoyancy effects due to spatial variation of

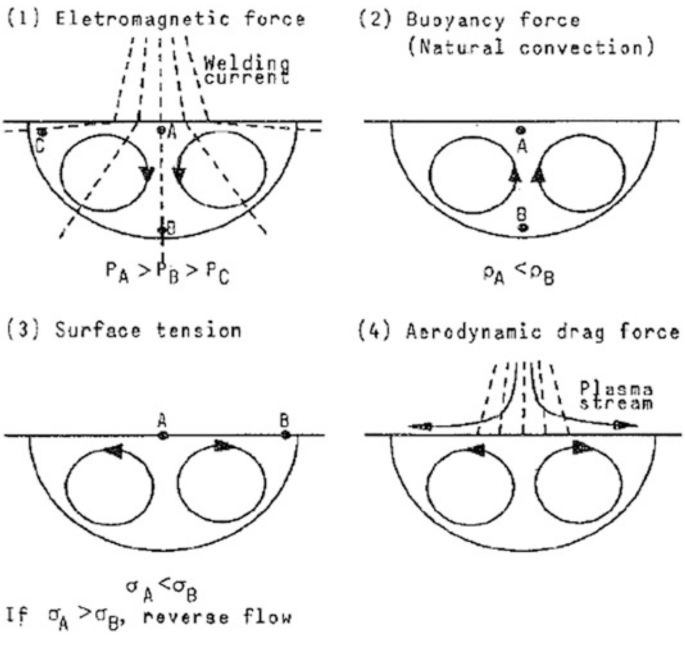

Fig. 2 Flow filed in the liquid pool induced by the four forces during arc welding (P_A, P_B and P_C are electromagnetic force induced pressure; ρ_A and ρ_B are buoyancy force; σ_A and σ_B are surface tension) [36]

Fig. 3 Different convective flow pattern produced by different temperature coefficient of surface tension [62]

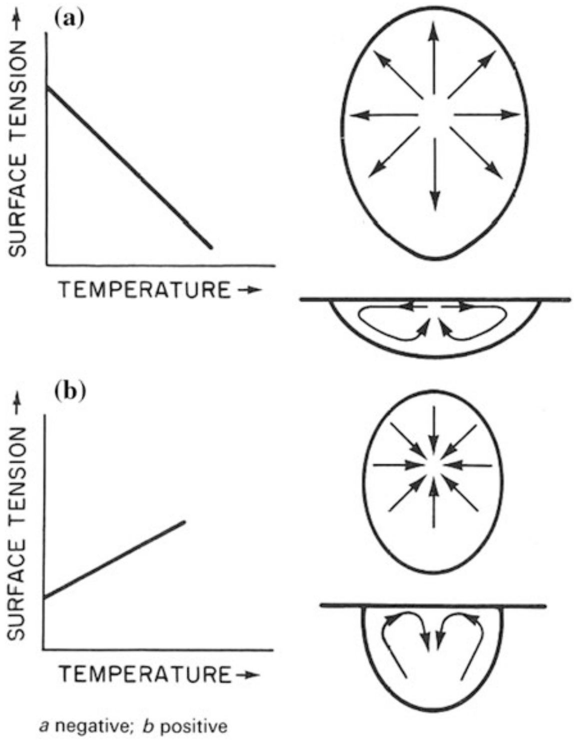

density of the liquid as a function of temperature and composition can provide convective flow. Electromagnetic forces are due to the divergent path of the current and the magnetic field that the current generates.

The reason that a shallow or deep penetration weld forms depends on the temperature coefficient of surface tension ($d\gamma/dT$). For pure metals and alloys, $d\gamma/dT$ is negative (Fig. 3). In a stationary arc weld, the highest temperature is in the middle of the weld pool. Therefore, the hot liquid flows outward, resulting in a shallow weld pool (Fig. 3). In the presence of surface-active elements such as phosphorous and sulfur and sometimes oxygen, the $d\gamma/dT$ is positive, resulting in the flow of the hot liquid inward, driving the hot liquid downward, and resulting in a deep weld pool. Figure 4 shows flow fields for pure iron resulting in a shallow weld pool and a deeper penetration with addition of oxygen. Depending on the interplay between various forms of driving force, the convective flow can be simple recirculation or a complex pattern with several convective cells (Fig. 4) [28, 36–38].

In the past three decades, most of the studies have concentrated on convective heat transfer, in particular, on the effect of spatial variation of surface tension on

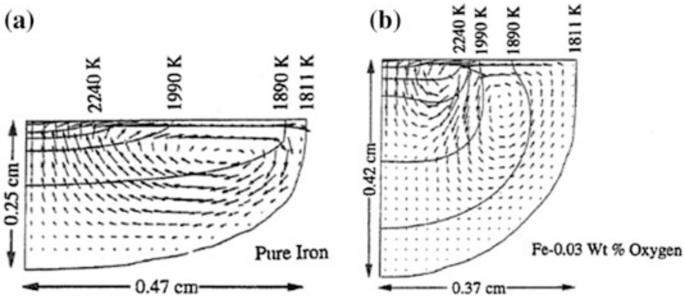

Fig. 4 Velocity and temperature fields for two different cases: **a** for pure iron and **b** for Fe-0.03 wt% oxygen [38]

weld penetration. For simplicity, most of the earlier models assumed stationary arc with a rigid weld pool surface. Recently, the models have been refined to incorporate realistic welding conditions such as deformable weld pool surface and moving heat source. In the last two decades, we have seen an enormous growth in understanding the physical process of welding. This is in part due to the speed and availability of computers. The introduction of massively parallel computers is expected to solve complex problems posed by intelligent weld manufacturing.

DebRoy et al. [39] have developed a computerized analysis for predicting heat transfer, phase changes, and fluid flow. They describe the use of modeling of the mushy zone using an ethology-porosity technique [39]. Figure 5 shows the computed convective flow of the weld part during arc welding. The color represents the temperature (in degrees kelvin), and the dotted lines show the liquid flow field. The two large loops shown near the surface of the pool are from Marangoni flow; the other loops below are due to electromagnetic effects [40].

The variable penetration during welding of different batches of a commercial alloy within a prescribed range has received considerable attention. Studies [39] have shown that knowledge of the interfacial phenomenon is the key for understanding and controlling weld penetration [17, 18, 28, 35–40]. Often the penetration

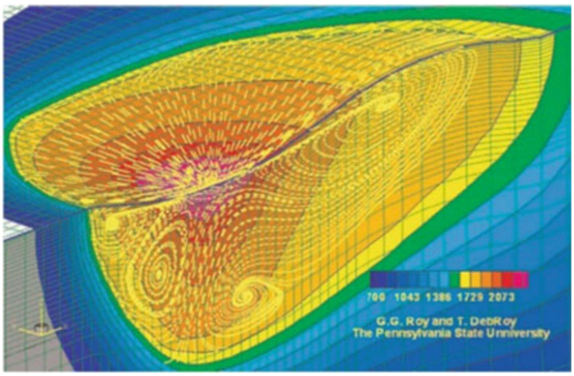

Fig. 5 Computed flow fields in a GTA weld pool. The color represents the temperature in the weld pool, and the dotted lines represent the liquid flow pattern. Two loops on the surface are from Marangoni flow (courtesy of Prof. DebRoy, Penn State University) (Color figure online)

is determined by the concentration of surface-active elements in the alloy [41–43]. This can affect the temperature/coefficient of surface tension and the resulting direction of fluid flow [34].

Weld penetration is an important consideration for weld automation. It is one of the parameters that need to be incorporated in the models. Weld penetration has been determined extensively by the physical feature of the weld pool such as weld pool oscillation and geometry [44–46].

2.2 Vaporization and Solution of Gas

During welding, the surface temperature of the weld pool is higher than the liquidus temperature of the alloy. In a high-energy-density process such as laser and electron beam welding, the temperature would exceed the boiling point of the alloy [47, 48]. Consequently, vaporization of the alloying elements can occur, changing the composition and hence changing the microstructure and the properties of the weld. DebRoy et al. have developed a computer model to describe the vaporization of the elements in a weld [49–51].

During welding, gases such as hydrogen, oxygen, and nitrogen dissolve in the liquid pool, causing pinholes and porosity. They also react with elements in the weld pool to form oxide and nitride inclusions [52]. Hydrogen causes hydrogen embrittlement, and nitrogen increases the yield strength and reduces ductility. Realistic modeling of hydrogen absorption and diffusion and their effects on hydrogen embrittlement is a challenge.

2.3 Artificial Neural Network Modeling

Two of the most important weld features in automated welding are weld pool geometry and penetration. Over the past three decades, several computational models have been developed for weld pool shape and penetration. The models have become more complex and sophisticated and require greater computational power. Although they are excellent tools for understanding the physical processes in welding, they are not available for the end users. An alternate process is the use of artificial neural network (ANN) [53]. A publication by Bhadeshia highlights the application of neural network in materials science [54]. Neural network models can be sophisticated, but they are limited to the experimental datasets on which they are based.

ANN has been used to solve problems in many areas of science and technology. The neural networks are modeled after the learning process in the human brain. Such models are empirically based and are capable of providing results rapidly. An example is the prediction of weld pool shape in a hybrid laser/arc process for which the physics of the process is not well known. Numerical models exist for laser or arc

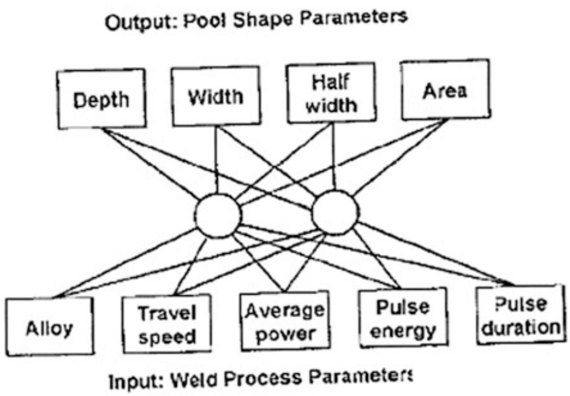

Fig. 6 Neural network architecture for predicting weld pool shape and penetration [53]

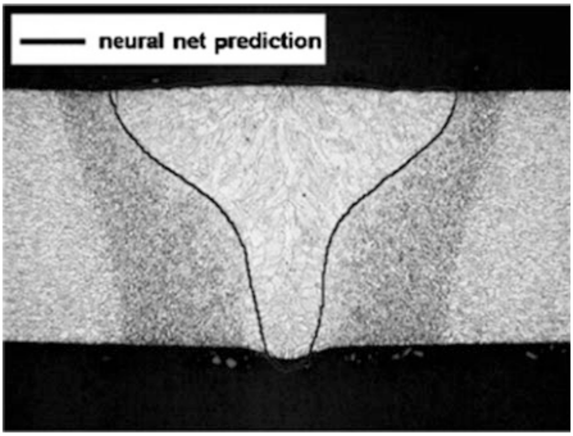

Fig. 7 Comparison of weld cross section predicted by neural network model and the actual weld pool [53]

welding processes. Other examples include prediction of the weld joint penetration based on the shape of the weld pool geometry [55] and real-time control of weld penetration based on real-time measurement of the weld pool geometry [56]. It is difficult to accurately model the hybrid process without knowing the physics of the process [53]. Figure 6 shows neural network architecture for laser/arc hybrid process; Fig. 7 shows prediction of an ANN model and the weld metal. The agreement is excellent. ANN modeling has been used for a wide variety of investigations [54, 57–60]. Sterjovski et al. have used ANNs for modeling the mechanical properties of steels in various applications [58] and for predicting diffusible hydrogen control and cracking susceptible in flux-covered arc welds [59]. Vitek et al. [60] have developed the Oak Ridge Ferrite Number (ORFN), a new model for predicting ferrite content in stainless steel welds. For the first time, ferrite content is predicted quantitatively as a function of alloy composition and cooling rate. The model is based on a neural network analysis of existing data supplemented with newly generated data.

3 Microstructure

As a welding heat source interacts with metal, three distinct regions can be identified, namely, fusion zone (FZ), heat affected zone (HAZ), and the base material (BM) (Fig. 8). The microstructural characteristics of the three regions control the properties and performance of the weld. A weldment is often the weakest link in the structure. During welding, various physical processes such as thermochemical reactions in the liquid, solidification, and solid-state transformation that occur in the weld metal control the microstructural development in the weld. Some fundamental knowledge of the effect of these physical processes on the microstructural development in the weld metal already exists. A review by Babu [61] examines various models for the development of microstructure in weldments. He analyzes the phase transformation in metals and alloys due to the weld thermal cycle experience during welding. The first event to occur when the weld pool cools is liquid transforming to solid and solid subsequently transforming to single-phase or multiple-phase structures through a solid-state reaction. The same is true of the HAZ except there is no melting in the HAZ. All these events are analyzed using computational thermodynamics (CT) models and computational kinetics (CK) models that relate to free energy of phases. The stability of the phases depends on the free energy of phases. Phases with high free energy are unstable; phases with low free energy are stable. The rate of phase change is related to diffusion and nucleation rate within the parent phase that leads to the product phase. However, a generalized integrated model encompassing our current understanding of the evaluation of microstructure is just emerging. Such models are needed in the design and successful development of intelligent weld manufacturing.

Most of our knowledge about weld metal solidification is derived from the extension of the knowledge of freezing of castings and single crystals in lower thermal gradients and at slower growth rates [62]. However, various physical processes that occur during the interaction of the heat source with the metal add a

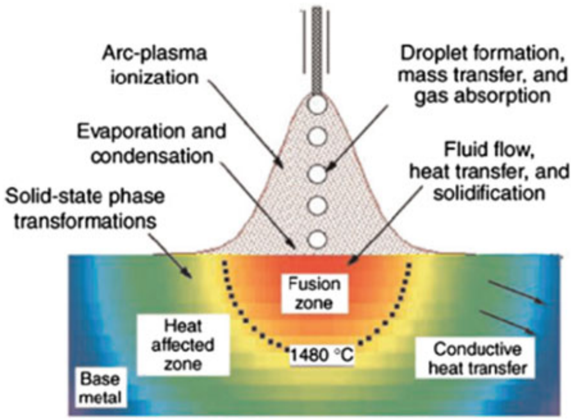

Fig. 8 Schematic illustration of interaction of heat source with metal and three regions of the weldment, namely FZ, HAZ and BM

new dimension to our understanding of weld metal solidification. Conventional theories of solidification over a broad range of conditions can be extended to understand weld pool solidification. In certain cases, because of rapid cooling rate effects, it is not unusual to observe nonequilibrium phases. Recent developments in the application of computational thermodynamics and kinetic models, studies of single-crystal welds and advanced characterization techniques have enhanced our understanding of weld pool solidification behavior. Advanced in situ characterization techniques such as synchrotron and neutron sources have enhanced our understanding of phase formation and formation of nonequilibrium phases [63, 64]. Other important factors are the dynamics of weld pool development and steady state geometry. Weld pool shape is important in the development of grain structure and the dendrite grain selection process [62].

Several fundamental aspects of solidification processes (nucleation, epitaxial growth, the growth selection process, growth kinetics, and microsegregation) must be understood to develop a basic model for solidification microstructure. In the FZ, the liquid metal transforms to solid. The size and shape of the grains, the distribution of inclusions, and the presence of defects such as hot cracks are controlled by the solidification behavior. Unlike the solidification of ingots and casting, solidification of a weld occurs without a nucleation barrier. No significant undercooling is required for the formation of the solid. Solidification occurs spontaneously by epitaxial growth on the partially melted grains.

Solidification microstructures in welds are often difficult to interpret and are commonly analyzed with the help of classical theories of nucleation and growth [62]. The development of microstructural features (morphology) of the solid in the weld is controlled by the shape of the solid/liquid interface and its stability. Stability of the interface is determined by the constitution and thermal conditions that exist at the interface. Theories have been developed for interface stability for equilibrium conditions at the interface for normal solidification or under extreme nonequilibrium conditions prevalent during rapid solidification [65, 66]. These theories can be extended to weld pool solidification. The parameters that determine the solidification microstructures in contrast are growth rate (R), thermal gradient (G) and undercooling (ΔT). It is well known that temperature gradient and growth rate are important in the combined form $G{\bullet}R$ or G/R. Depending on the conditions, growth of the solid can be planar, cellular, or dendritic. A dendrite isolated from the liquid is shown in Fig. 9 [67]. Weld metal grain structure is predominantly determined by the base metal grain structure [68]. Crystallographic effects and welding conditions have been found to influence this grain structure. Often the grains during the weld pool solidification tend to grow along a crystallographic direction that is easy growth direction. For cubic metals the easy growth directions are <100>. Conditions for growth are optimal when one of the easy growth directions coincides with the heat flow direction. Therefore, during welding among the randomly oriented grains in the polycrystalline base metal, those that are favorably oriented will continue to grow. Unfortunately for the unfavorably oriented grains, the growth will terminate, thus leading to a grain growth selection process. This grain anisotropy

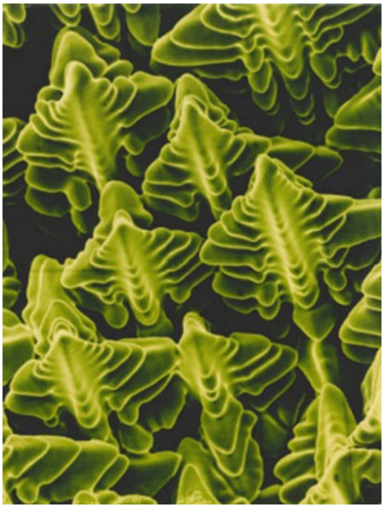

Fig. 9 Scanning electron micrograph showing the features of dendrite structure that develops in a nickel-based superalloy [67]

was clearly demonstrated by the work of Rappaz and David using a Fe-Ni-Cr single-crystal weld [69].

Another significant aspect of weld pool solidification is solute redistribution. During welding, the extensive solute redistribution that occurs in the weld pool results in segregation that can adversely affect weldability, microstructure, and properties. Only recently some attention is being given to this important aspect of weld pool solidification [70–73]. A great deal of work needs to be done in this area. Availability of software packages to calculate multicomponent phase diagrams will make it easier to determine models for solute redistribution in multicomponent alloys.

In most of the cases, both the weld metal and the HAZ go through a solid-state transformation. The transformation and the resulting microstructures control the properties. Hence modeling of solid-state transformations in the weld is important to developing an integrated model [61]. In addition to phase transformation in the weldment, an integrated model should address grain growth, precipitations, coarsening, and solute redistribution. The transformations can be grouped in four classes: (1) phase changes involving diffusional processes, (2) solid-state processes involving grain growth, (3) phase changes involving displacement transformation, and (4) phase changes such as spinodal decompositions. The driving force for grain growth and coarsening relates to minimization of interfacial energy. Analytical models and Monte-Carlo simulations are routinely carried out to analyze these phenomena [62, 72, 73].

In most of the alloy systems, the development of microstructure depends on a series of events. In the case of low-alloy steels, the sequences of events that occur are shown in Fig. 10 [74]. The model for microstructure development in low-alloy steel has a number of sub-models recorded on the sequences of events that the weld metal goes through. In low-alloy steel welds the properties of steel are improved by maximizing acicular ferrite phase constituent in the microstructure. Although

Fig. 10 The sequential formation of various phase changes that occur during cooling of the low-alloy steel weldment [74]

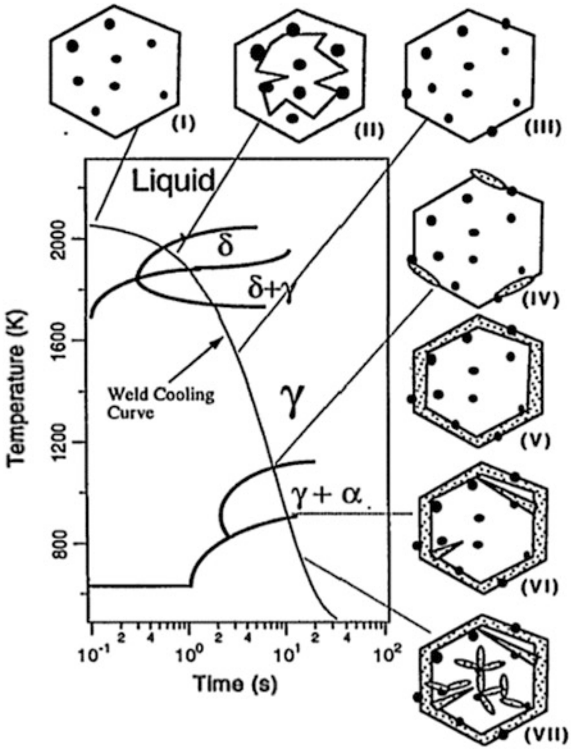

acicular ferrite forms from austenite, the feasibility of acicular ferrite formation depends on the presence of inclusions and austenite grain size. The microstructure evolution is controlled by the sequential formation of various phases as shown in Fig. 10.

4 Sensors, Intelligent Control, and Automation

Intelligent control and automation are critical elements of ICWE and intelligent weld manufacturing. As welding technology matures, there will be a steady decrease in manual welding. For increased accuracy and productivity, future welding operations will require welding systems with effective adaptive control [75]. Adaptive weld control is a closed loop approach that relies on measurements of relevant physical characteristics of the weld pool as the feedback and feedback control algorithms that decide how to respond to the feedback. Chen has discussed the framework for research and technology for intelligent weld manufacturing [76, 77]. This includes computer vision systems for visual feedback sensing, and control, neural network modeling of the process dynamics, and fuzzy logic and neurons self-leaving learning for control algorithms of arc welding. The machinery, controls, and materials needed for ICWE are becoming more sophisticated, and the industry to produce them is growing. The needed sensors, controls, and control software, robots, and automatic machines are constantly being invented and integrated.

Zhang [78] has provided a comprehensive analysis on why a welding process should be monitored and how they can be effectively monitored for control. In his analysis, welding process is treated as a system, argued as a complex system, analyzed for its uncertainty and the necessity for monitoring and control, and is artificially decomposed for effective monitoring for control.

Naidu et al. [79] have conducted a survey of automatic control strategies for gas metal arc welding (GMAW) process. His results provide the status of feedback control techniques as applied to the GMAW process. Naidu's report describes the current state of sensing and control techniques involved such as classical control, neutral network, fuzzy logic control, adaptive control, and expert systems.

One of the critical elements of adaptive control is sensors. The function of the sensors is to provide information to the control system to face the necessary changes to the process to produce parts with highest integrity or at least meeting the specification despite variations in manufacturing conditions. Significant advances are being made in the development of sensors [44, 45, 80–86]. The sensors that are available currently are optical, arc, infrared, acoustic, and ultrasonic. For example, novel optical sensors have been used for observing welding operations and processes. Some have the resolution to view the weld puddle and to clearly see the solidification substructure (dendrites) formed on the pool surface [84].

For weld penetration, den Ouden [44] was able to correlate the weld pool oscillation frequency to the weld penetration, and Zhang [45] was able to correlate the weld pool geometry to the weld penetration. Zhang and his group have developed a real-time sensing and control device to predict weld penetration based on weld pool surface reflectivity [85]. In that system, the intensity of the weld pool surface reflectivity increases as the weld penetration increases. That correlation has been used to control the quality of the weld.

Seam tracking is a critical element in adaptive welding. Dilthey [84] developed a "through the arc" sensing device for seam tracking. Cook et al. [86] developed a seam-tracking control system based on fuzzy logic that tracks seams during pulsed GMAW. To produce welds with good quality and specified geometry, it is necessary to control the positioning of the welding torch. The method of using the arc itself as a sensor to sense and control the process is called "through the arc" tracking. Dilthey designed and implemented a fuzzy logic through-the-arc control system. The system provides an excellent real-time feedback control system for welding machine R&D.

Lv et al. [87] have developed a real-time arc length control and weld pool surface height prediction method by acoustic sensing and segmented self-adaptive proportional–integral–derivative (PID) controller during pulsed gas tungsten arc welding (GTAW). The experimental validation has demonstrated the feasibility of weld process control through the acoustic signals from the welding arc.

Recent developments using infrared sensing have demonstrated its potential for seam tracking [88]. Although these types of sensors are critical for ultimate process control, significant emphasis should be placed on sensors for microstructure and properties [89]. The ultimate goal of the adaptive control is to regulate the process to make welds with desired quality, performance, and productivity. The current trend is to use an emerging tool known as “intelligent control.” This will enable one to choose a desirable end factor such as property, defect control, or productivity instead of process parameters such as current, voltage, or speed to provide for appropriate control of the process.

Another intelligent welding approach is automated pass planning. Welders often take a fairly long time when they use multipass welding to weld large joints. With appropriate automated pass planning, the sequence and number of passes can be optimized, and a welding robot can complete the welding process in a much shorter time [90].

Significant advances are being made to produce parts intelligently through the development of sensors and feedback control systems. Neural networks are being applied for seam tracking. Cook et al. have developed neural network fuzzy logic control system [75].

Tight coupling of the welding variables imposes limitations on the extent of control that can be exercised. Cook et al. [86] discuss decoupling of welding variables for improved automatic control. The process considered includes GTAW, and GMAW. From the point of view of control, the process or the process variant that gives the most decoupling of the control parameters is desired because it would make it easier for control system design and would increase the range of control over the variable parameters.

Sadek and Drews [91] have investigated intelligent systems for welding process automation. They evaluated the idea and the implementation of two distinct multiserver systems for automated manufacturing based on a parallel computing architecture. They have shown that multiserver systems with distributed architectures offer considerable advantages over standard bus-based systems.

5 Friction Stir Welding

The four key elements to intelligent weld manufacturing that enable the production of high-quality welds with increased productivity, which again are process and process modeling, microstructure, properties, and process control and automation, are not unique to arc welding. Other forms of welding, including welding that occurs in the solid-state, are guided by these principles as well. One form of solid-state welding, Friction Stir Welding (FSW), in particular, has garnered attention from researchers in recent years as a highly dynamic, thermomechanical process with a rich potential for research endeavors into process modeling, control, and intelligent welding. FSW is relatively a new welding process developed by Wayne Thomas at The Welding Institute (TWI), Cambridge, UK [92, 93]. It is a solid-state process and involves plunging and rotating a tool at the joint to be made between two plates and traversing along the joint line. Heat generated due to

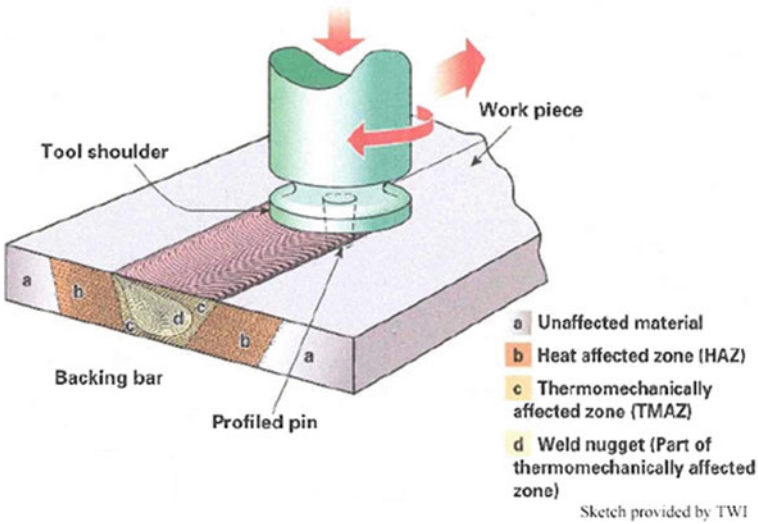

Fig. 11 Schematic of friction stir welding process showing the interaction of the tool with the material (courtesy of TWI)

friction and plastic deformation softens the workpiece, and flow of the metal brings about a metallurgical bond. A schematic of the process is shown in Fig. 11. It has great potential for applications in automotive, aerospace, transportation, and energy industries. While the fundamental underlying theories and methods for modeling of the weld process, conducting process development, and performing analysis of weld properties and microstructure are perhaps not significantly different, specific techniques are tailored to meet the unique details, conditions, and constraints of the FSW process. With respect to process modeling, researchers have approached FSW from both analytical and numerical modeling perspectives. DebRoy and his group [94–97] have carried out extensive modeling and simulation studies of FSW processes related to 3D heat and material flow, torque and power, tool durability, and dissimilar materials joining. Nunes developed a widely utilized analytical model [98].

5.1 Control and Automation of FSW

In order to achieve high-quality FSW, a well-understood framework for control and automation is imperative, and the variables to control and automate the process are different from that of commercial fusion welding processes. Cook [99, 100] and Smith [101, 102] were among the first to document the challenges and opportunities associated with robotic FSW. One of the most important relationships to control is relative tool-workpiece positioning, i.e. the tool plunge depth. This relationship can impact weld penetration, defect formation, tool wear, heat generation, and resulting weld properties. Position control alone can be inadequate due to inconsistent workpiece dimensions, thermal expansion, robot deflection due to high process forces, or the welding of complex geometries. For these reasons, force or torque control in FSW has become important for researchers and manufacturers, with Longhurst et al. [103–107] contributing significantly in this area, along with many others [108–110]. Force sensing is thus an important capability as well, with sensing typically accomplished via load cell [111–114], but Smith et al. [115] demonstrated that axial force can also be sensed via measurement of robot motor currents and use of the Jacobian [116] relationship.

5.2 *Advanced Sensing and Intelligent FSW*

Given the success of 'through-the-arc' sensing techniques, 'through-the-tool' sensing has been explored in FSW as a means of similarly improving process characteristics. Smith et al. [117] and De Backer et al. [118] documented problems in robotic FSW, such as planned-path deviations caused by high forces. While, Soron et al. [119] and Fleming et al. [120] showed that it is possible to compensate for deviations based on force sensing (and the use of vision systems is an option too [118, 121]), novel 'through-the-tool' joint tracking capabilities have been successfully demonstrated [122–124]. Intelligent FSW describes the correlation of process output data to welding outcomes to augment the knowledge of researchers and to improve process efficiency. Boldsaikhan et al. have been significant contributors in this area, with a focus on defect detection and with the use of artificial neural networks [125–128]. Both Fleming et al. [129] and Gibson et al. [130] used dimensional reduction techniques to classify weld quality, and defect formation caused by tool wear has been detected as well [131]. Additional efforts in intelligent FSW by Bhowmick [132], Jene et al. [133], Britos et al. [134–136], and Burford et al. [137] have included successful attempts to map process input parameters to welding outcomes and to correlate force signatures with weld features.

6 Integration of Weld Models

To develop an intelligent weld manufacturing, all the four principal elements defined by various sub-models must be integrated. Integration of all the four principal elements mentioned early with sub-models is a very challenging and a monumental task. This can be achieved but it would be costly and time consuming. Such integration is essential to the development of intelligent weld manufacturing. Microstructural evolution in low-alloy steel welds is described as an example. Evolution of microstructures in a low-alloy weld is not defined by a single event. It occurs over a range of temperatures. First, as the liquid metal cools, the oxygen in the liquid steel reacts with the deoxidizing element in the liquid to form an oxide inclusion that acts as a nucleating agent for solid δ-ferrite. This occurs over a range of temperatures. Figure 9 shows schematic of continuous cooling transformation showing the development of weld metal microstructure in low-alloy steels. Upon cooling, δ-ferrite forms and with further cooling the δ-ferrite transforms to austenite and austenite transforms to γ-ferrite with different morphologies [84]. These changes occur sequentially. Physical processes that occur at elevated temperatures, such as plasma–liquid metal interaction, also affect the ultimate microstructure obtained. Vaporization and dissolution of gases change the composition of the liquid. This change in composition that occurs at elevated temperatures affects the microstructural evolution at lower temperatures. Therefore, an integrated model is necessary to predict the evolution of microstructure in the low-alloy steel welds.

Integrated process models (thermal models) and microstructure models were developed in the nineties [89, 91, 138, 139]. However, integration of the integrated process models with the microstructure models has been achieved only recently [39, 89]. The ability to predict microstructural evolution in weld metal is critical to the development of intelligent manufacturing. Using a CT and CK framework, Babu [61] describes the phase stability and rates of change during phase transformation during a weld thermal cycle. The work carried out at universities, national laboratories, and industrial research organizations in the United States, Europe, and Asia laid the foundation for developing an integrated thermomechanical and microstructure models. These developments were summarized by Kirkaldy [138] in a block diagram (Fig. 12). First the thermal model simulates three-dimensional (3D) temperature distribution as a function of process parameters and time [61]. The materials model uses thermal cycle data to predict the microstructure evolution and its effect on transient mechanical properties. The transient change in thermal and mechanical properties is fed into a finite-element structural model to predict plastic stress distribution. That information is used for prediction of final properties, residual stress, and distortion.

Pavlyk et al. [140] modeled the coupling of simulated weld-solidification microstructure with a macroscopic fluid flow model. Several microstructural simulation techniques have been developed. Pavlyk et al. used a coupled CA-FDM technique to simulate weld dendrite structure. They determined solidification conditions during weld pool solidification. As in the case of accurate physical models, calculations are carried out at microstructural spatial resolution.

DebRoy et al. [39] carried out weld microstructure calculations from the fundamentals of transport phenomena in the arc welding of low-alloy steel welds. A 3D transient heat and fluid flow model was used to calculate the cooling rates in a manual GTA weld of different compositions of low-alloy steel welds. The weld metal composition was used to calculate the time temperature and transformation (TTT) diagram. These TTT diagrams were converted to continuous cooling transformation (CCT) diagrams. Cooling rates were coupled to TTT diagram to obtain CCT diagrams, using which the various microstructural constituents were determined.

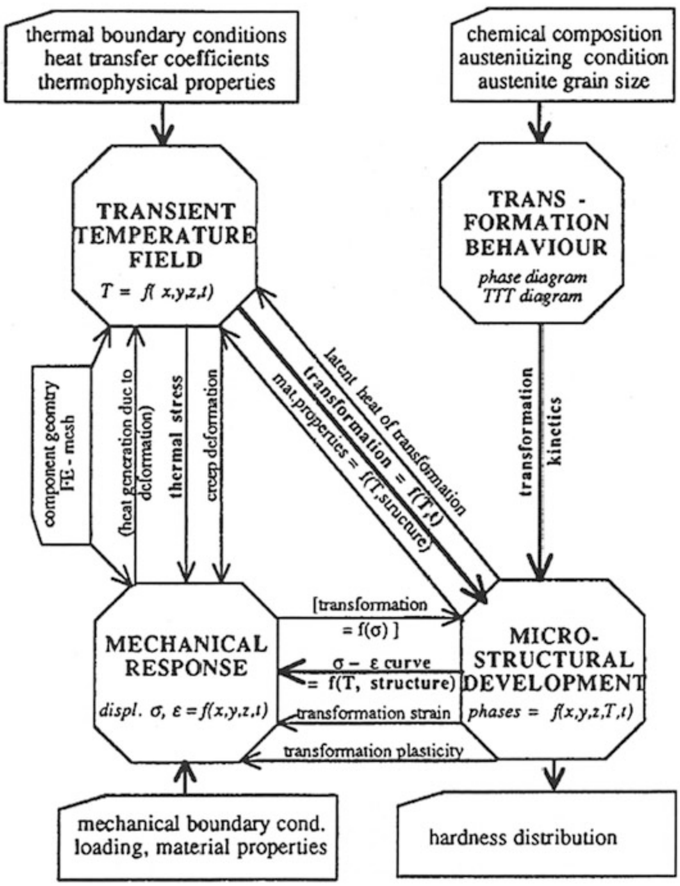

Fig. 12 Block diagram describing integrated weld modeling methodology by Kirkaldy [138]

Feng et al. [141, 142] developed modeling approach based on ICWE to predict the mechanical behavior of resistance spot welds. They devised an incrementally coupled electric-thermal-mechanical-metallurgical model to predict weld microstructure and properties as a function of steel chemistry and welding conditions. The resulting microstructure and property distribution in a spot weld is then used in a damage-mechanics-based structural model to predict the strength and failure of resistance spot welds of advanced high-strength steels for automotive applications. With such an ICWE-based model, it is possible to realistically simulate the effects of welding conditions and steel chemistry on the highly heterogeneous microstructure distribution (Fig. 13) as well as the deformation, strength, and failure of the weld as function of microstructure and property distributions (Fig. 14).

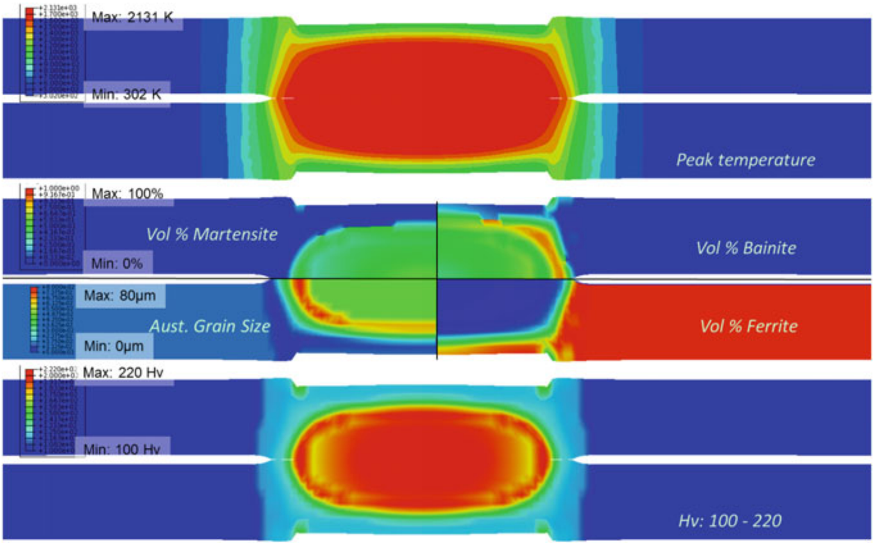

Fig. 13 Prediction of weld nugget formation, grain growth, microstructural constituents and resulting microhardness distribution of a DQSK steel during resistance spot welding [142]

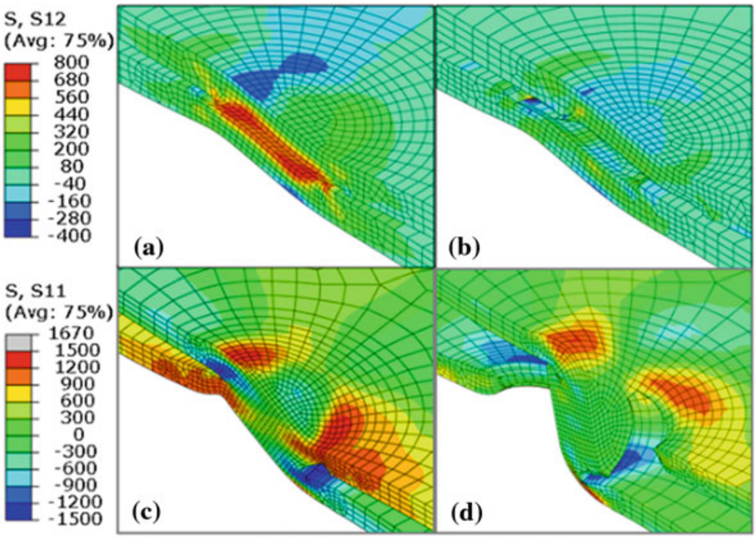

Fig. 14 Predicted failure mode changes of resistance spot weld of a boron steel [142]

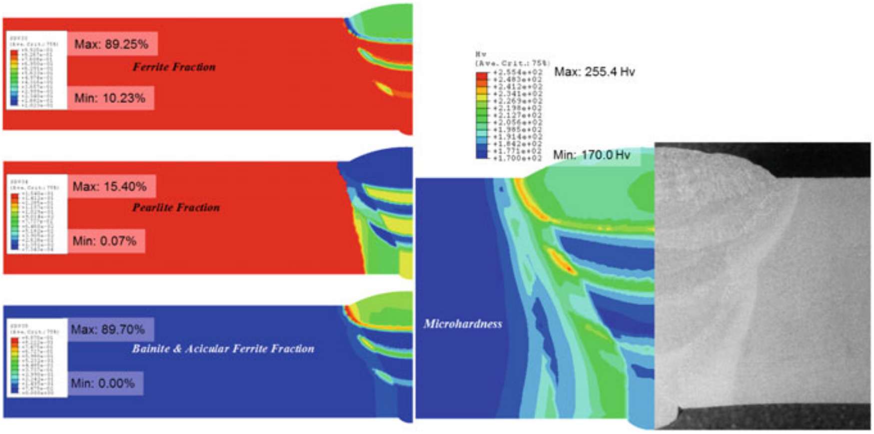

Fig. 15 Prediction of microstructure constituents and resulting microhardness distribution in a X65 pipeline steel [143]

The ICWE modeling approach taken by Feng et al. is also applicable to arc welding processes and friction stir welding of steels and aluminum alloys [143, 144]. In the case of a multipass X65 pipeline steel, the coarse grain HAZ exhibited elevated hardness due to formation of different microstructure constituents in solid-state phase transformation as a result of grain growth in the coarse grain heat affected zone (CGHAZ) (Fig. 15). The effect of multiple welding thermal cycles on the microstructure is also faithfully simulated. Such a model has been used to optimize the welding process conditions and weld filler metal chemistry to tailor the weld microstructure and weld residual stress in high-strength steel to eliminate hydrogen-induced cracking, improve weld fatigue life, and minimize weld distortions [145].

Feng et al. [144] demonstrated that the ICWE model is capable of predicting the effect of welding process conditions on the microstructure, strength, and deformation and failure of friction stir welded Al6061 alloys. The effect of welding speed on the temperature, microstructure, strength, and residual stress can be predicted with high fidelity (Fig. 16). Such a model has been used to guide the welding process development to improve the properties of friction stir welds.

Doyle and Conrady describe a program for the design, construction, and demonstration of a prototype programmable automated welding system [146]. The program, known as the programmable automated welding system (PAWS), was sponsored by the US Naval Surface Warfare Center. Doyle and Conrady developed a system with control capabilities to accept, arbitrate, and reach its inputs from multiple sensors.

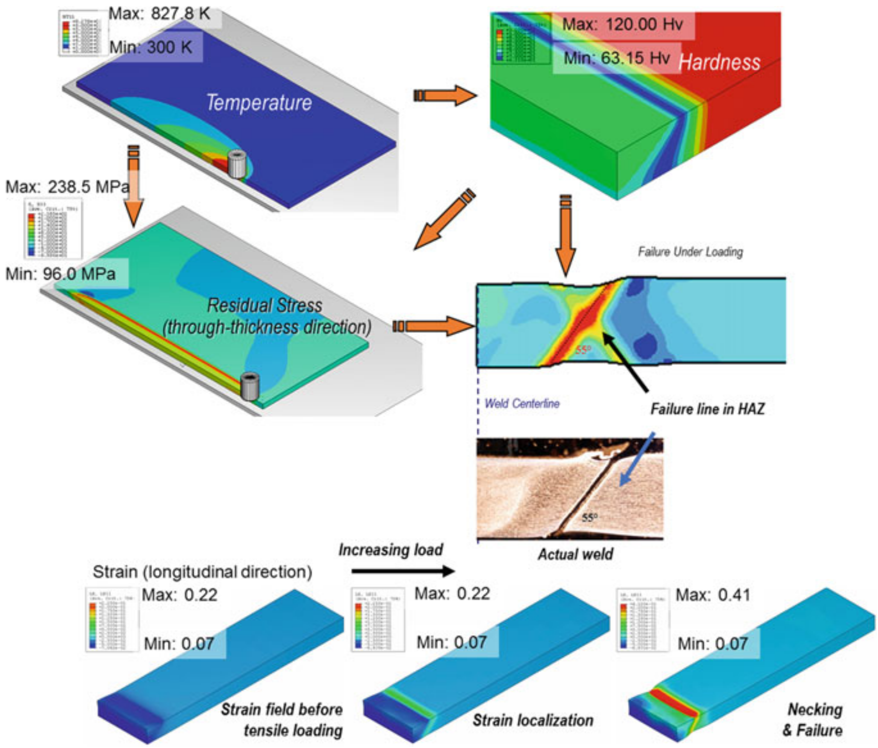

Fig. 16 Integrated multiphysics simulations provide realistic predictions of performance and failure of Al 6061 friction stir welds [144]

7 Conclusion

Intelligent weld manufacturing involves sensing and control of the heat source, position, weld defect formation, and ultimately microstructure and properties. The ultimate goal of intelligent weld manufacturing is to produce high-quality welds with increased productivity. Computational modeling and simulation are key parts of intelligent weld manufacturing. Computational modeling of weld manufacturing involves solution to a problem with many highly coupled and nonlinear variables. It requires a multidisciplinary ICWE modeling approach to cover and connect four major elements—processes, control and automation, microstructure, and properties—for intelligent weld manufacturing.

Intelligent weld manufacturing is at a crossroads. We are at a point in the research at which major breakthroughs are possible to enable us to attain the ultimate goal of intelligent weld manufacturing. Yet significant challenges remain. In ICWE, it is now possible to perform a detailed simulation with sufficient fidelity to achieve design and manufacturing optimization of structural welding of vehicles or welding of nuclear reactor components. However, this type of weld simulation is very time consuming with today's computers. It often takes weeks or months to perform such a detailed simulation. Research and development to utilize high-performance computing systems would be a potential direction to drastically reduce the computational time (by 103 or more) for intelligent weld manufacturing. Artificial intelligence and deep machine learning would be another potential solution to integrate ICWE into intelligent weld manufacturing.

Acknowledgements The authors would like to acknowledge Ms. Shirin Badlani for her help in preparing the manuscript. We would also like to acknowledge Prof. Yuming Zhang (University of Kentucky) and Prof. G.E. Cook (Vanderbilt University) for their review and valuable comments. This material is based upon work supported by the U.S. Department of Energy, Office of Science, Office of Basic Energy Sciences, Office of Nuclear Energy, and Office of Energy Efficiency and Renewable Energy under a prime contract with Oak Ridge National Laboratory (ORNL). ORNL is managed by UT-Battelle, LLC for the U.S. Department of Energy under Contract DE-AC05-00OR22725.

References

1. Drews P, Starke G (1994) Welding in the century of information technology. Weld. World 34:1–20
2. Dilthey U, Stein L (1992) Robot system for arc welding-current position and future trends. Weld. Cutting 8:E150–E152
3. Pan JL (1999) A survey of welding sciences in 21st century. In: Proceedings of 9th Chinese Welding Conference, vol 1, CWC, Tianjin, China, p D001-D017
4. Trailer (1995) Manufacturer depends on robotic welding to boost production. Weld J 74(7): 49–51
5. Tarn TJ, Chen SB, Zhou CJ (2004) Robotic welding, intelligence and automation. Springer, Berlin
6. Tarn TJ, Chen SB, Zhou CJ (2007) Robotic welding, intelligence and automation. Springer, Berlin
7. Tarn TJ, Chen SB, Fang G (2011) Robotic welding, intelligence and automation. Springer, Berlin
8. Chen SB (2015) Robotic welding, intelligence and automation, advances in intelligent systems and computing. Springer, Singapore
9. Chen SB, Lou YJ, Wu L et al (2000) Intelligent methodology for sensing, modeling and control of pulsed GTAW: Part l, bead-on-plate welding. Weld. J. 79(6):151s–163s
10. David SA, Vitek JM. International trends in welding research (1986, 1989, 1992, 1995, 1998, 2001, 2004, 2008, 2010), ASM Intl, Material Park, OH
11. Cerjak H, Bhadesha HKDH. Mathematical modeling of weld phenomenon (1993, 1995, 1997, 1998, 2000, 2002), Springer, Berlin
12. Friedman E (1978) Analysis of weld puddle distortion and its effect on penetration. Weld. J. 57(6):161s–166s
13. Jhaveri P, Moffat WG, Adams CM (1962) The effect of plate thickness and radiation on heat flow in welding and cutting. Weld. J. 41(1):12s–16s

14. Nippes EF, Merrill LL, Savage WF (1949) Cooling rates in arc welds in ½ plates. Weld. J. 28(12):556s–564s
15. Oreper GM, Szekely J (1984) Heat-flow and fluid-flow phenomena in weld pools. Fluid. Mech. 147:53–79
16. Tsai NS, Eagar TW (1984) The distribution of heat source in arc welding. In: Proceedings of the international conference modeling of casting and welding process II, AIME, New York, p 317
17. Kou S, Sun DK (1985) Fluid flow and weld penetration in stationary arc welds. Metall. Trans. A 16:203–213
18. Kou S, Wang YH (1986) Weld pool convection and its effects. Weld. J. 65:63s–70s
19. Sundell RE, Correa SM, Harris LP, et al (1986) GE Report 86SRD013
20. Zacharia T, Eraslan AH, Aidun DK (1988) Modeling of non-autogenous welding. Weld. J. 67(1):18s–27s
21. Zacharia T, Eraslan AH, Aidun DK et al (1989) Three-dimensional transient model for arc welding process. Metall. Trans. B 20:645–659
22. Zacharia T, David SA, Vitek JM et al (1989) Weld pool development during GTA and laser beam welding of type 304 stainless steel, Part I—theoretical analysis. Weld. J. 68(2):499s–509s
23. Zacharia T, David SA, Vitek JM et al (1991) Computational modeling of stationary gas-tungsten-arc weld pools and comparison to stainless steel 304 experimental results. Metall Trans B 22B:243–257
24. Choo RT, Szekely J (1991) The effect of gas shear stress on Marangoni flows in arc welding. Weld. J. 70:223s–233s
25. David SA, DebRoy T (1992) Current issues and problems in welding science. Science 257:497–502
26. Zacharia T, Bjeria MA, Tmorovic SC (1993) International conference on modeling and control of joining processes. MCJP, Orlando, FL
27. Miller R, DebRoy T (1990) Energy absorption by metal-vapour-dominated plasma during carbon dioxide laser welding of steels. J. Appl. Phys. 68:2045–2050
28. Rosenthal D (1941) Mathematical theory of heat distribution during welding. Weld. J. 20 (5):220s–234s
29. Rosenthal D (1946) The theory of moving sources of heat and its application to metal treatments. Trans. ASME 68:849–866
30. Zacharia T, Vitek JM, Goldak JA et al (1995) Modeling of fundamental phenomena in welds. Model. Simul. Mater. Sci. Eng. 2:265–288
31. Kou S, Le Y (1983) Three-dimensional heat flow and solidification during the autogenous GTA welding of aluminum plate. Metall. Trans. A 14A:2243–2253
32. Chan C, Mazumder J, Chen MM (1984) A two-dimensional transient model for convection in laser melted pool. Metall. Trans. A 15A:2175–2184
33. Paul A, DebRoy T (1988) Free surface flow and heat transfer in conduction mode laser welding. Metall. Trans. B 19B:851–858
34. Zacharia T, David SA, Vitek JM et al (1989) Heat transfer during Nd-YAG pulsed laser welding and its effect on solidification structure of austenitic stainless-steels. Metall. Trans. A 20A:957–967
35. Zacharia T, David SA, Vitek JM (1991) Effect of convection in weld pool development. In: Proceedings of symposium on the metals science and joining, Cincinnati, OH, pp 257–263
36. Matsunawa A (1992) Modeling of heat and fluid flow in arc welding. International Trends in Welding Research, ASM International, Materials Park, OH
37. Kou S, Le Y (1988) Welding parameters and the grain-structure of weld metal—a thermodynamic consideration. Metall. Trans. 19(4):1075–1082
38. Zacharia T, David SA, Vitek JM et al (1991) Effect of evaporation and temperature-dependent material properties on weld pool development. Metall. Trans. B 22B:233–241

39. Mundra K, DebRoy T, Keller KM (1996) Numerical prediction of fluid flow and heat transfer in welding with a moving heat source. Numer. Heat Transfer Part A 29(2):115–129
40. DebRoy T (1995) Role of interfacial phenomena in numerical analysis of weldability, mathematical modelling of weld phenomena II. Dissertation, The Institute of Materials, London, pp 3–21
41. Heiple CR, Roper JR (1982) Mechanism for minor element effect on GTA fusion zone geometry. Weld. J. 61(4):97s–102s
42. Heiple CR, Burgardt P (1985) Effects of SO_2 shielding gas additions on GTA weld shape. Weld. J. 64(6):159s–162s
43. Szekely J, Preper GM, McKelliget J (1986) Proceedings of the engineering foundation conference on the modeling and control of welding and casting processes. Springer, Santa Barbara, CA, USA
44. Hu B, den Ouden G (1999) Weld penetration sensing and control during GTA welding using weld pool oscillation. Trends in Welding Research, ASM International, Materials Park, OH
45. Zhang YM, Li L (1999) Controlling joint penetration based on weld pool geometry. Trends in Welding Research, ASM International, Materials Park, OH
46. Zhang YM, Wu L, Walcott BL et al (1993) Determining joint penetration in GTAW with vision sensing of weld face geometry. Weld. J. 72(10):463s–469s
47. Batanov VA, Bunkin FV, Prokhorov AM et al (1973) Evaporation of metallic targets caused by intense optical radiation. Sov. Phys. 36:311–322
48. Chan CL, Mazumder J (1987) One-dimensional steady-state model for damage by vaporization and liquid expulsion due to laser-material interaction. J. Appl. Phys. 62 (11):4576–4586
49. Khan PA, DebRoy T (1984) Alloying element vaporization and weld pool temperature during laser-welding of ANSI 202 stainless-steel. Metall. Trans. B 15(4):641–644
50. Mundra K, DebRoy T (1993) Calculation of weld metal composition change in high-power conduction mode carbon-dioxide laser-welded stainless-steels. Metall. Trans. B 24(1): 145–155
51. Mundra K, DebRoy T (1993) Role of thermophysical properties in weld pool modeling. Weld. J. 72(1):1s–9s
52. Banerjee A, Onneby C, DebRoy T, et al (1993) Nitrogen dissolution in the weld pool. Trends in Welding Research, ASM International, Materials Park, OH
53. Vitek JM, Iskander YS, Oblow EM, et al (1999) Neural network modeling of pulsed-laser weld pool shape in aluminum alloy welds. Trends in Welding Research, ASM International, Materials Park, OH
54. Bhadeshia HKDH (2009) Neural networks and information in materials science. Stat. Anal. Data Min. 1:296–305
55. Kovacevic R, Zhang YM (1997) Neurofuzzy model-based weld fusion state estimation. IEEE Control Syst. Mag. 17(2):30–42
56. Zhang YM, Kovacevic R (1998) Neurofuzzy model-based predictive control of weld fusion zone geometry. IEEE Trans. Fuzzy Syst. 6(3):389–401
57. Vitek JM, Iskander YS, Oblow EM, et al (1999) Neural network model for predicting ferrite number in stainless steel welds. In: Trends in Weld Research, ASM International, Material Park, OH
58. Sterjovski Z, Nolan D, Carpenter MR et al (2005) Artificial neural networks for modeling the mechanical properties of steels in various applications. J. Mater. Process. Technol. 170:536–544
59. Sterjovski Z, Pitrun MD, Nolan D et al (2007) Artificial neural networks for predicting diffusible hydrogen content and cracking susceptibility in rutile flux-cored arc welds. J. Mater. Process. Technol. 184(1–3):420–427
60. Vitek JM, David SA, Hinman CR (2003) Improved ferrite number prediction model that accounts for cooling rate effects—part 1: model development—details of a prediction model based on a neural network system of analysis are described. Weld. J. 82(1):10s–17s

61. Babu SS (2009) Thermodynamic and kinetic models for describing microstructure evolution during joining of metals and alloys. Int. Mater. Rev. 54(6):333–367
62. David SA, Vitek JM (1989) Correlation between solidification parameters and weld microstructures. Int. Mater. Rev. 34(5):213–245
63. Elmer JW, Wong J, Ressler T (2000) In-situ observations of phase transformations during solidification and cooling of austenitic stainless-steel welds using time-resolved X-ray diffraction. Scr. Mater. 43(8):751–757
64. Elmer JW, Wong J, Ressler T (2001) Spatially resolved X-ray diffraction mapping of phase transformations in the heat-affected zone of carbon-manganese steel arc welds. Metall. Mater. Trans. A 32(5):1175–1187
65. Flemingo MC (1974) Solidification processing. McGraw Hill, NY
66. Kurz W, Fisher DJ (1986) Fundamentals of solidification. Trans SEM Publication, Acdemana Dort, Switzerland
67. David SA, Siefert JA, DuPont JN et al (2015) Weldability and weld performance of candidate nickel base super-alloys for advanced ultra-supercritical fossil power plants part I: fundamentals. Sci. Technol. Weld. Joining 20(7):532–552
68. Savage WF, Lundin CD, Aronson A (1965) Weld metal solidifications mechanics. Weld. J. 44(4):s175
69. Rappaz M, David SA, Vitek JM et al (1990) Analysis of solidification microstructures in Fe-Ni-Cr single-crystal welds. Metall. Trans. A 21A:1767–1782
70. Brooks JA, Baskes NT, Grelich FA (1991) Solidification modeling and solid-state transformations in high-energy density stainless-steel welds. Metall. Trans. A 22(4):915–926
71. Lippold JC, Savage W (1980) Modeling of casting and welding processes. Warrendale, PA
72. David SA, Vitek JM (1993) Mathematical modeling of weld Phenomena. The Institute of Materials, London, pp 41–59
73. Radhakrishnan B, Zacharia T (1995) Simulation of curvature-driven grain-growth by using a modified Monte-Carlo algorithm. Metall. Mater. Trans. 26:167–180
74. Babu SS, David SA (2002) Inclusion formation and microstructure evolution in low alloy steel welds. ISIJ Int. 42(12):1344–1353
75. Cook GE, Andersen K, Barrathe KJ (1990) Feedback and adaptive control in welding. In: Proceedings of Recent Trends in Welding Technology, ASM Intl, Materials Park, OH
76. Chen SB, Lou YJ, Wu L et al (2000) Intelligent methodology for sensing, modeling and control of pulsed GTAW: part I—bead-on-plate welding. Weld. J. 79(6):151s–163s
77. Chen SB, Lou YJ, Wu L et al (2000) Intelligent methodology for sensing, modeling and control of pulsed GTAW: part II—Butt joint welding. Weld. J. 79(6):164s–174s
78. Zhang YM (2008) An analysis of welding process monitoring and control. Real-Time Weld Process Monitoring, Cambridge, England, pp. 1–11
79. Naidu DS, Moore KL (1999) Automatic control strategies for gas metal arc welding: a status survey. Trends in Welding Research, ASM International Materials Park, OH
80. Richardson RW, Gutow DA, Anderson RA et al (1984) Coaxial arc weld pool viewing for process monitoring and control. Weld. J. 63(3):43–49
81. Bolstad J (1987) Advances in automation for precision arc welding. In: Proceedings of Edison Welding Institute, EWI, Columbus, OH
82. Bolikel C, Mazumder J (1992) Optical diagnostics of laser weld pool free surface. In: 3rd International Conference on Trends in Welding Research, ASM International, Materials Park, OH
83. Nagarajan S, Banderjee P, Chen WH et al (1991) Control of the welding process using infrared sensors. IEEE Trans. Robot. Autom. 8(1):86–93
84. Dilthey U, Gollnick J (1999) Through-the-arc sensing in GMA-welding with high speed rotating torch. In: Proceedings of Trends in Welding Research, ASM International, Materials Park, OH
85. Chen J, Chen J, Feng Z, et al (2016) Dynamic evolution of the weld pool reflection during weld penetration development. In: IEEE International Conference on Advanced Intelligent Mechatronics, IEEE, Banff, Albert, Canada

86. Barnett RJ, Cook GE, Damrongsak D et al (1999) Through-the-arc sensing and control in pulsed gas tungsten metal arc welding. Trends in Welding Research, ASM International, Material Park, OH
87. Lv N, Zhong J, Chen H et al (2014) Real-time control of welding penetration during robotic GTAW dynamical process by audio sensing of arc length. Int. J. Adv. Manuf. Technol. 74 (1–4):235–249
88. Chin BA, Madsen NH, Goodling JS (1983) Infrared thermography for sensing the weld process. Weld. J. 62(9):227s–234s
89. Babu SS, David SA, Vitek JM et al (1995) Phase transformations and microstructure development in low alloy steel welds. In: Proceedings of International Symposium in Phase Transformation during Thermomechanical Processing of Steels, Vancouver, Canada
90. Yan SJ, Ong SK, Nee AYC (2016) Optimal pass planning for robotic welding of large-dimension joints with deep grooves. Procedia CIRP 56:188–192
91. Sadek Alfredo CA, Drews P (2006) Intelligent systems for welding process automation. Braz. Soc. Sci. Eng. 26(1):25–29
92. Thomas WM (1991) Friction stir butt welding. International Patent Application No PCT/GB92 Patent Application No. 9125978.8
93. Thomas WM, Nicholas ED (1997) Friction stir welding and friction extrusion of aluminium and its alloys. In: 3rd World Congress on Aluminium, Limassol, Cyprus
94. DebRoy T, De A, Bhadeshia HKDH et al (2012) Tool durability maps for friction stir welding of an aluminum alloy. In: Proceedings of the Royal Society A—Mathematical Physical and Engineering Sciences, vol. 468, pp. 3552–3570
95. Manvatkar VD, Arora A, De A et al (2012) Neural network models of peak temperature, torque, traverse force, bending stress and maximum shear stress during friction stir welding. Sci. Technol. Weld. Joining 17(6):460–466
96. Nandan R, Roy GG, Lienert TJ et al (2007) Three-dimensional heat and material flow during friction stir welding of mild steel. Acta Mater. 55:883–895
97. Nandan R, Prabu B, De A et al (2007) Improving reliability of heat transfer and fluid flow calculations during friction stir welding of dissimilar aluminum alloys. Weld. J. 86 (10):313s–322s
98. Nunes AC, Bernstein EI, McClure JC (2000) A rotating plug model for friction stir welding. In: Proceedings of the 81st American Welding Society Convention, AWSC, Chicago, IL
99. Cook GE, Smartt H, Mitchell J et al (2003) Controlling robotic friction stir welding. Weld. J. 8:28–34
100. Cook GE, Crawford R, Clark D et al (2004) Robotic friction stir welding. Ind. Robot 31 (1):55–63
101. Smith C (2007) Robots and machines for friction stir welding/processing. Friction Stir Weld. Process. 11:219–233
102. Smith C (2000) Robotic friction stir welding using a standard industrial robot. In: Proceedings of the 2nd International Symposium on Friction Stir Welding, TWI, Cambridge, UK
103. Longhurst WR (2009) Force control of friction stir welding. Dissertation, Vanderbilt University
104. Longhurst WR, Strauss AM, Cook GE et al (2010) Investigation of force controlled friction stir welding for manufacturing and automation. Proc. Inst. Mech. Eng. Part B: J Eng Manuf. 224(6):937–949
105. Longhurst WR, Strauss AM, Cook GE (2011) Identification of the key enablers for force control of robotic friction stir welding. J. Manuf. Sci. Eng. 133(3):31008–31019
106. Longhurst WR, Strauss AM, Cook GE et al (2010) Torque control of friction stir welding for manufacturing and automation. Int. J. Adv. Manuf. Technol. 51:905–913
107. Longhurst WR, Cox CD, Gibson BT et al (2014) Applied torque control of friction stir welding using motor current as feedback. Proc. Inst. Mech. Eng. Part B: J. Eng. Manuf. 228 (8):947–958

108. Gibson BT, Lammlein DH, Prater TJ et al (2014) Friction stir welding: process, automation, and control. J. Manuf. Process. 16(1):56–73
109. Fehrenbacher A, Duffie NA, Ferrier NJ et al (2011) Toward automation of friction stir welding through temperature measurement and closed-loop control. J. Manuf. Sci. Eng. 133 (5):1–12
110. Cederqvist L, Garpinger O, Oberg T (2012) Control of temperature, power input, and tool depth during FSW of copper canisters. In: Proceedings of the 9th International Symposium on Friction Stir Welding, TWI, Cambridge, UK
111. Blignault C, Hattingh DG, Kruger GH et al (2008) Friction stir weld process evaluation by multi-axial transducer. Measurement 41:32–43
112. Gibson BT (2011) Custom low-cost force measurement methods in friction stir welding. Dissertation, Vanderbilt University
113. Gibson BT, Cox CD, Longhurst WR et al (2012) Exploiting robotic link deflection for low-cost force measurement in manufacturing. Measurement 45:140–142
114. Gibson BT, Cox CD, Aguilar JR et al (2012) Low-cost wireless force sensor design with applications in friction stir welding. In: Proceedings of 9th International Trends in Welding Research Conference, RTWRC, Chicago, IL
115. Smith C, Hinrichs J, Crusan W (2003) Robotic friction stir welding: state-of-the-art. In: Proceedings of the 4th International Symposium on Friction Stir Welding, TWI, Cambridge, UK
116. Craig J (2005) Introduction to Robotics Mechanics and Control. Pearson Prentice Hall
117. Smith CB, Schroeder K, Fehrenbacher A (2012) An automated path planning and programming system with real-time adaptive control for friction stir processing of cast surfaces. In: Proceedings of the 9th International Symposium on Friction Stir Welding, TWI, Cambridge, UK
118. De Backer J, Christiansson AK, Oqueka J et al (2012) Investigation of path compensation methods for robotic friction stir welding. Ind. Robot Int. J. 39(6):601–608
119. Soron M, De Backer J, Christiansson AK et al (2010) A local model for online path corrections in friction stir welding. In Proceedings of Friction Stir Welding and Processing Conference, FSWPC, Lille, France
120. Fleming PA, Lammlein DH, Wilkes DM et al (2009) Misalignment detection and enabling of seam tracking for friction stir welding. Sci. Technol. Weld. Joining 14(1):93–96
121. Christner B, Hansen M, Skinner M et al (2003) Friction stir welding system development for thin gauge aerospace structures. In: Proceedings of the 4th International Symposium on Friction Stir Welding, TWI, Cambridge, UK
122. Fleming PA, Hendricks CE, Wilkes DM et al (2009) Automatic seam-tracking of friction stir welded T-joints. Int. J. Adv. Manuf. Technol. 45:490–495
123. Fleming PA, Hendricks CE, Cook GE et al (2010) Seam-tracking for friction stir welded lap joints. J. Mater. Eng. Perform. 19(8):1128–1132
124. Gibson BT, Cox CD, Ballun MC et al (2014) Automatic tracking of blind sealant paths in friction stir lap joining. J. Aircr. 51(3):824–832
125. Boldsaikhan E, Corwin E, Logar A et al (2006) Neural network evaluation of weld quality using FSW feedback data. In: Proceedings of the 6th International Symposium on FSW, FSW, Saint-Sauver, Canada
126. Boldsaikhan E (2008) The use of feedback forces for non-destructive evaluation of friction stir welding. Dissertation, South Dakota School of Mines and Technology
127. Boldsaikhan E, Corwin E, Logar A et al (2011) The use of neural network and discrete Fourier transform for real-time evaluation of friction stir welding. Appl. Soft Comput. 11:4839–4846
128. Boldsaikhan E, Bharat J, Logar A (2010) A phase space approach to detecting volumetric defects in friction stir welding. In: Proceedings of the 8th International Symposium on Friction Stir Welding, TWI, Cambridge, UK
129. Fleming PA, Lammlein DH, Wilkes DM et al (2008) In-process gap detection in friction stir welding. Sens. Rev. 28(1):62–67

130. Gibson BT, Wilkes DM, Cook GE et al (2013) In-Process detection of faying surface sealant application flaws in friction stir welding. J. Aircr. 50(2):567–575
131. Gibson BT, Tang W, Peterson AG et al (2017) Evaluating the potential for remote in-process monitoring of tool wear in friction stir welding of stainless steel. J. Manuf. Sci. Eng. Accepted manuscript published online, July 13
132. Bhowmick A (2010) Prediction of friction stir weld quality using self-organized maps. Dissertation, Aukland University of Technology, Aukland, New Zealand
133. Jene T, Dobman G, Wagner G (2008) Monitoring of the friction stir welding process to describe parameter effects on joint quality. Weld. World 52(9–10):47–53
134. Britos P, Widener C, Brown J et al (2009) Correlation between ultrasonic phased array and feedback force analysis of friction stir welds. Friction Stir Welding and Processing V, Springer, Berlin
135. Britos P, Widener C, Boldsaikhan E et al (2010) Probability of detection analysis of NDT methods for friction stir welded panels. In: Proceedings of the 8th International Symposium on Friction Stir Welding, TWI, Cambridge, UK
136. Britos P (2010) Probability of detection in friction stir welding using non-destructive evaluation techniques. Dissertation, Wichita State University
137. Burford D, Britos P, Boldsaikhan E (2010) Evaluation of friction stir weld process and properties for aerospace application: e-NDE for friction stir processes. In: Proceedings of FAA Joint Advanced Materials & Structures (JAMS) 6th Annual Technical Review Meeting, JAMS, Seattle, USA
138. Kirkaldy JS (1991) Diffusion-controlled phase-transformations in steels—theory and applications. Scand. J. Metall. 20:50–61
139. Mundra BK, DebRoy T, Babu SS et al (1997) Weld metal microstructure calculations from fundamentals of transport phenomena in the arc welding of low-alloy steels. Weld. J. 76(4): s163–s171
140. Pavlyk V, Dithey U (2004) Simulation of weld solidification microstructure and its coupling to the macroscopic heat and fluid flow modelling. Model. Simul. Mate. Sci. Eng. 12: S33–S45
141. Feng Z, Babu SS, Riemer BW et al (2001) Modeling of resistance spot welds: process and performance. Weld. World 45:18–24
142. Zheng L, Feng Z, Simunovic S et al (2013) Integrated computational model for resistance spot welds in auto-body crashworthiness CAE: process, properties, and performance. In: Proceedings of 2nd World Congress on Integrated Computational Materials Engineering, WCICME, Salt Lake City, Utah, USA
143. Chauhan V, Feng Z (2002) Gas transmission pipeline girth weld residual stresses and the effects of hydrotesting. In: Proceedings of 4th International Pipeline Conference, ASME, Calgary, Canada, pp. 381–388
144. Feng Z, Wang XL, David SA et al (2007) Modelling of residual stresses and property distributions in friction stir welds of aluminum alloy 6061-T6. Sci. Technol. Weld. Joining 12:348–356
145. Feng Z, David SA, Tzelepis DA et al (2015) US Patent Application Pub No 2016/0228998A1
146. Manly TD, Doyle TE (1993) Arc hydrogen monitoring for synergic GMAW. In: Proceedings of International Trends in Welding Science and Technology, ASM International Materials Park, OH